Effect of Soret and Dufour on Unsteady MHD Jerry flow past a vertical porous plate with suction and chemical reaction

[1]A.K. Shukla∗, [2]Shubham Kumar Dube , [3]Mohammad Suleman Quraishi

[1]Assistant Professor in Mathematics, [2]Research Scholar, [3]Assistant Professor
[1,2]Department of Mathematics RSKD PG College Jaunpur-222001, India
[3]Department of Applied Sciences, Jahangirabad Institute of Technology, Barabanki, Uttar Pradesh, India.

***Abstract*— In this study, we looked at how modifications in the Soret and Dufour effects affected the magnetic fluid flow across a vertical porous plate with a first order chemical reaction in Jeffery MHD (magneto-hydrodynamics) fluid flow. Regulating partial differential equations have been used to explain the mathematical model of the flow field. The Crank-Nicolson implicit finite difference approach has been used to numerically solve non-dimensionalized flow field governing equations. With the use of graphs and tables, the impacts of non-dimensional factors on the concentration, temperature, and velocity profiles have been investigated. Table has also been used to observe fluctuations in factors like skin friction, the Nusselt number, and the Sherwood number in relation to other parameters.**

***Index Terms*—: Jeffery flow, Crank-Nicolson Method, Soret and Dufour effects and Chemical reaction.**

I. Introduction

In the literature reviewed past years, only the Newtonian fluid model was used for all experiments. Very little research has been done to examine how non-Newtonian fluids flow in porous-walled channels and tubes, despite the fact that the majority of industrial and biological fluids are non-Newtonian and the classical Newton's law of viscosity fails to describe the complex rheological properties of non-Newtonian fluids. One non-Newtonian fluid model that has drawn attention from researchers is the Jeffrey fluid model, which is thought to be a superior model for physiological fluids. Unsteady MHD Jeffery flow across a vertical porous plate with Soret-Dufour and first order chemical reaction has attracted the interest of many mathematicians. In recent years, it has become crucial to examine how mass transfer affects both Newtonian and non-Newtonian fluids. Numerous industries use heat transmission through radiation, including solar energy, semiconductor wafer processing, the production of transient crystals, energy transfer in furnaces, etc. Engines and combustion chambers are designed to run at higher temperatures to boost thermal efficiency. Nadeem et al. [1] has investigated the effects of thermal radiation on nano-fluid towards a stretching sheet with convective boundary conditions. Ibrahim et al. [2] projected their aim on Williamson nano-fluid flow in the presence of thermal radiation. Oztop and Selimefendegin [3] employed the finite element method to find out a numerical solution of MHD mixed convection in a flexible-walled and nanofluid filled the lid-derived cavity with volumetric heat generation. Kumar and Rajput [4] investigated the effect of radiation on MHD flow past an impulsively started vertical plate with variable heat and mass transfer. Ahmad et al. [5]. Kharabela et al.[7] worked on higher-order chemical reactions on MHD nanofluid flow with slip boundary conditions. Katagiri Srihari [6], Soret, Dufour and Hall effects on unsteady MHD flow past a semi infinite vertical plate by the presence of heat source Matta and Gajjela [8] have analysed the order of chemical reaction and convective boundary conditions on effects on micropolar fluid over a stretching sheet. Usman et al.[9] studied MHD free convective flow with thermal radiation and chemical reaction effects in the presence of variable suction. Rahman [10] explored the combined effect of internal heat generation and higher-order chemical reaction on the non-Dercian forced convective flow of a viscous incompressible fluid with variable viscosity and thermal conductivity over a stretching surface embedded in a porous medium. T. Hayat, et al. [11] , MHD flow of Jeffrey liquid due to a nonlinear radially stretched sheet in presence of Newtonian heating. M. Eswara Rao & S. Sreenadh [12], MHD Boundary Layer Flow of Jeffrey Fluid over a Stretching/Shrinking Sheet through Porous Medium. T. Hayat et al. [13], Simultaneous effects of melting heat and internal heat generation instagnation point flow of Jeffrey fluid towards a nonlinear stretching surface with variable thickness. M.A. Rana et al. [14], Three-dimensional Couette flow of a Jeffrey fluid along periodic injection/suction. M.A. Imran [15], MHD fractional Jeffrey's fluid flow in the presence of thermo diffusion, thermal radiation effects with first order chemical reaction and uniform heat flux. T. Hayat et al. [16], Radiative Flow of Jeffrey Fluid Through a Convectively Heated Stretching Cylinder. K. Das et al. [17], Radiative flow of MHD Jeffrey fluid past a stretching sheet with surface slip and melting heat Transfer. M.M. Bhatti & M. Ali Abbas [18], Simultaneous effects of slip and MHD on peristaltic blood flow of Jeffrey fluid model through a porous Medium. S. Sreenadh et al. [19], Peristaltic pumping of a power – Law fluid in contact with a Jeffrey fluid in an inclined channel with permeable walls. S. Farooq et al. [20], Magneto hydrodynamic peristalsis of variable viscosity Jeffrey liquid with heat and mass transfer. K. Venkateswara et al. [21], Unsteady MHD Mixed Convection Flow of Jeffrey Fluid Past a Radiating Inclined Permeable Moving Plate in the Presence of thermophoresis Heat Generation and Chemical Reaction. D. Dastagiri Babu et al. [22], Multivariate Jeffrey Fluid Flow past a Vertical Plate through Porous Medium.

Motivating from the above research work and the various possible industrial applications of the engineering fields, It is a great interest in the investigation of unsteady MHD Jeffery flow through a vertical porous plate with Soret-Dufour and first order chemical reaction. The effect of different parameters on velocity, temperature, mass transfer, shearing stress, local surface heat, and mass flux are being observed by solving numerically using Crank-Nicolson finite difference method for the governing equations of flow field and effects of appropriate parameters.

II. Mathematical Model of the problem

Consideration has been given to the flow of a viscous, incompressible Jeffery fluid in a boundary layer over a permeable, vertical plate submerged in a porous medium. Let's assume that the plate heats up at $\overline{T}_w$ and concentration $\overline{C}_w$. This model takes into account Soret-Dufour effects and first order chemical reactions in the flow variable. The plate is considered infinite in $\overline{x}$ –axis direction and $\overline{y}$-axis normal to the plate. $\frac{\partial \overline{u}}{\partial \overline{x}}$ is negligible in equation of continuity because flow direction is vertically upward. In starting; $\overline{t} \le 0$, we assumed that the plate and fluid are at the same temperature and concentration. For $\overline{t} \ge 0$, the plate moves with velocity u_0 and concentration and temperature increase exponentially with time. The induced magnetic field is neglected because transversely applied magnetic field and magnetic Reynold's number are small. In the direction of $\overline{y}$-axis, a magnetic field of uniform strength B_0 is considered. According to usual Boussinesq's approximation the governing equations and boundary conditions of this model are given as:

Equation of Continuity **:**

$$\frac{\partial \overline{v}}{\partial \overline{y}} = 0 \quad \Rightarrow \quad \overline{v} = -v_0(constant)$$

Momentum equation:

$$\frac{\partial \overline{u}}{\partial \overline{t}} + \overline{v}\frac{\partial \overline{u}}{\partial \overline{y}} = \left(\frac{\nu}{1+\lambda}\right)\frac{\partial^2 \overline{u}}{\partial \overline{y}^2} + g\beta_1(\overline{T} - \overline{T}_\infty) + g\beta_2(\overline{C} - \overline{C}_\infty) - \frac{\sigma B_0^{\,2}\overline{u}}{\rho} - \nu\frac{\overline{u}}{\overline{K}}$$

Energy equation**:**

$$\rho_\infty C_p\left(\frac{\partial \overline{T}}{\partial \overline{t}} + \overline{v}\frac{\partial \overline{T}}{\partial \overline{y}}\right) = k\frac{\partial^2 \overline{T}}{\partial \overline{y}^2} - \frac{\partial q_r}{\partial \overline{y}} + \frac{\rho D_m K_T}{c_s}\frac{\partial^2 \overline{C}}{\partial \overline{y}^2}$$

Concentration equation:

$$\frac{\partial \overline{C}}{\partial \overline{t}} + \overline{v}\frac{\partial \overline{C}}{\partial \overline{y}} = D\frac{\partial^2 \overline{C}}{\partial \overline{y}^2} + \frac{D_m K_T}{T_m}\frac{\partial^2 \overline{T}}{\partial \overline{y}^2} - k_r\left(\overline{C} - \overline{C}_\infty\right)$$

where $\overline{T}$ and $\overline{C}$ are dimensional temperature and concentration $\overline{C_w}$ and $\overline{T_w}$ are concentration and temperature of free stream, in Equation 4; $k_r(\overline{C} - \overline{C_\infty})$ has been introduced for first order chemical reaction, k_r is chemical reaction constant, β_1 is volumetric coefficient of thermal expansion, β_2 is coefficient of volume expansion for mass transfer, q_r is radiative heat along $\overline{y}$-axis, ν is kinematic viscosity and T_m is mean fluid temperature, $\overline{v}$ is suction velocity along $\overline{y}$-axis, $\overline{K}$ is permeability of porous medium, σ is electrical conductivity, D_m is molecular diffusivity, g is acceleration due to gravity, K_T is thermal diffusion ratio, μ is viscosity, ρ is fluid density, k is thermal conductivity of fluid, C_p is specific heat at constant pressure.

The boundary conditions for this model are assumed as:

$$\left.\begin{array}{llllll}
\overline{t} \le 0; & \overline{u} = 0, & v = -v_0 & \overline{T} = \overline{T}_\infty, & \overline{C} = \overline{C}_\infty & \forall\, \overline{y} \\
\overline{t} > 0; & \overline{u} = u_0, & \overline{T} = \overline{T}_\infty + (\overline{T}_w - \overline{T}_\infty)e^{-At}, & & \overline{C} = \overline{C}_\infty + (\overline{C}_w - \overline{C}_\infty)e^{-At} \quad at & \overline{y} = 0 \\
 & \overline{u} \to 0, & \overline{T} \to \overline{T}_\infty, & & \overline{C} \to \overline{C}_\infty \quad as & \overline{y} \to \infty
\end{array}\right\}$$

Where $A = \frac{v_0^{\,2}}{\nu}$

Roseland explained the term radiative heat flux approximately as

$$q_r = -\frac{4\sigma_{st}}{3a_m}\frac{\partial \overline{T}^4}{\partial \overline{y}^4} \tag{6}$$

Here Stefan Boltzmann constant and absorption coefficient are σ_{st} and a_m respectively.

In this case temperature differences are very-very small within flow, such that $\overline{T}^4$ can be expressed linearly with temperature. It is realized by expanding in a Taylor series about T_∞' and neglecting higher order terms, so

$$\bar{T}^4 \cong 4\bar{T}_\infty^{\,3}\bar{T} - 3\bar{T}_\infty^{\,4}$$

With the help of equations (6) and (7), we write the equation (3) in this way

$$\rho_\infty C_p\left(\frac{\partial \bar{T}}{\partial \bar{t}} + \bar{v}\frac{\partial \bar{T}}{\partial \bar{y}}\right) = k\frac{\partial^2 \bar{T}}{\partial \bar{y}^2} + \frac{16\bar{T}_\infty^{\,3}\sigma_{st}}{3a_m}\frac{\partial^2 \bar{T}}{\partial \bar{y}^2} + \frac{\rho D_m K_T}{c_s}\frac{\partial^2 \bar{C}}{\partial \bar{y}^2}$$

Let us introduce the following dimensionless quantities

$$\left.\begin{aligned}
&u = \frac{\bar{u}}{u_0}, t = \frac{\bar{t}\nu_0^{\,2}}{\nu}, y = \frac{\bar{y}\nu_0}{\nu}, \theta = \frac{\bar{T}-\bar{T}_\infty}{\bar{T}_w-\bar{T}_\infty}, C = \frac{\bar{C}-\bar{C}_\infty}{\bar{C}_w-\bar{C}_\infty},\\
&G_m = \frac{\nu g\beta_c(\bar{C}_w-\bar{C}_\infty)}{u_0\nu_0^{\,2}}, G_r = \frac{\nu\, g\beta(\bar{T}_w-\bar{T}_\infty)}{u_0\nu_0^{\,2}}, K = \frac{\nu_0^{\,2}}{\nu^2}\bar{K},\\
&S_c = \frac{\nu}{D}, P_r = \frac{\mu C_p}{k}, M = \frac{\sigma B_0^{\,2}\nu}{\rho\nu_0^{\,2}}, R = \frac{4\sigma\bar{T}_\infty^{\,3}}{k_m k}, K_r = \frac{k_r\nu}{\nu_0^{\,2}},\\
&D_u = \frac{D_m K_T(\bar{C}_w-\bar{C}_\infty)}{c_s c_p\nu(\bar{T}_w-\bar{T}_\infty)}, S_r = \frac{D_m K_T(\bar{T}_w-\bar{T}_\infty)}{T_m\nu(\bar{C}_w-\bar{C}_\infty)}, A = \frac{\nu_0^{\,2}}{\nu}
\end{aligned}\right\}$$

Using substitutions of Equation 9, we get non-dimensional form of partial differential Equations 2, 8 and 4 respectively

$$\frac{\partial u}{\partial t} - \frac{\partial u}{\partial y} = \left(\frac{1}{1+\lambda}\right)\frac{\partial^2 u}{\partial y^2} + G_r\theta + G_m C - \left(M + \frac{1}{K}\right)u$$

$$\frac{\partial \theta}{\partial t} - \frac{\partial \theta}{\partial y} = \frac{1}{P_r}\left(1 + \frac{4R}{3}\right)\frac{\partial^2 \theta}{\partial y^2} + D_u\frac{\partial^2 C}{\partial y^2}$$

$$\frac{\partial C}{\partial t} - \frac{\partial C}{\partial y} = \frac{1}{S_c}\frac{\partial^2 C}{\partial y^2} + S_r\frac{\partial^2 \theta}{\partial y^2} - K_r C$$

With initial and boundary conditions

$$\left.\begin{aligned}
&t \le 0; \quad u = 0, \quad \theta = 0, \quad C = 0 \quad \forall y\\
&t > 0; \quad u = 1, \quad \theta = e^{-t}, \quad C = e^{-t} \quad at\ y = 0\\
&u \to 0, \quad \theta \to 0, \quad C \to 0 \quad as\ y \to \infty
\end{aligned}\right\} \qquad (13)$$

The degree of practical interest includes the Skin friction coefficients τ, local Nusselt Nu, and local Sherwood Sh numbers are given as follows:

$$\tau = -\left(\frac{\partial u}{\partial y}\right)_{y=0}, N_u = -\left(\frac{\partial \theta}{\partial y}\right)_{y=0}, Sh = -\left(\frac{\partial C}{\partial y}\right)_{y=0} \qquad (14)$$

III. Numerical Method of Solution

Exact solution of system of partial differential Equations 10, 11 and 12 with boundary conditions given by Equation 13 are impossible. So, these equations we have solved by Crank-Nicolson implicit finite difference method. The Crank-Nicolson finite difference implicit method is a second order method in time ($o(\Delta t^2)$) and space, hence no restriction on space and time steps, that

is, the method is unconditionally stable. The computation is executed for Δy = 0.1, Δt = 0.001 and procedure is repeated till y = 4. Equations 10, 11 and 12 are expressed as

$$\frac{u_{i,j+1}-u_{i,j}}{\Delta t}-\frac{u_{i+1,j}-u_{i,j}}{\Delta y}=\left(\frac{1}{1+\lambda}\right)\frac{u_{i-1,j}-2u_{i,j}+u_{i+1,j}+u_{i-1,j+1}-2u_{i,j+1}+u_{i+1,j+1}}{2(\Delta y)^2}$$

$$+G_r\left(\frac{\theta_{i,j+1}+\theta_{i,j}}{2}\right)+G_m\left(\frac{C_{i,j+1}+C_{i,j}}{2}\right)-\left(M+\frac{1}{K}\right)\left(\frac{u_{i,j+1}+u_{i,j}}{2}\right) \quad \square\square\square\square$$

$$\frac{\theta_{i,j+1}-\theta_{i,j}}{\Delta t}-\frac{\theta_{i+1,j}-\theta_{i,j}}{\Delta y}=\frac{1}{P_r}\left(1+\frac{4R}{3}\right)\left(\frac{\theta_{i-1,j}-2\theta_{i,j}+\theta_{i+1,j}+\theta_{i-1,j+1}-2\theta_{i,j+1}+\theta_{i+1,j+1}}{2(\Delta y)^2}\right) \quad \square\square\square\square$$

$$+D_u\left(\frac{C_{i-1,j}-2C_{i,j}+C_{i+1,j}+C_{i-1,j+1}-2C_{i,j+1}+C_{i+1,j+1}}{2(\Delta y)^2}\right)$$

$$\frac{C_{i,j+1}-C_{i,j}}{\Delta t}-\frac{C_{i+1,j}-C_{i,j}}{\Delta y}=\frac{1}{S_C}\left(\frac{C_{i-1,j}-2C_{i,j}+C_{i+1,j}+C_{i-1,j+1}-2C_{i,j+1}+C_{i+1,j+1}}{2(\Delta y)^2}\right) \quad \square\square\square\square$$

$$+S_r\left(\frac{\theta_{i-1,j}-2\theta_{i,j}+\theta_{i+1,j}+\theta_{i-1,j+1}-2\theta_{i,j+1}+\theta_{i+1,j+1}}{2(\Delta y)^2}\right)+K_r\left(\frac{C_{i,j+1}+C_{i,j}}{2}\right) \quad \square\square\square\square\square\square\square$$

Initial and boundary conditions are also rewritten as:

$$u_{i,0}=0,\quad \theta_{i,0}=0,\quad C_{i,0}=0 \qquad \forall i$$

$$u_{0,j}=1,\quad \theta_{0,j}=e^{-j\Delta t},\quad C_{0,j}=e^{-j\Delta t} \qquad \forall j \quad \square\square\square\square$$

$$u_{l,j}\to 0,\quad \theta_{l,j}\to 0,\quad C_{l,j}\to 0 \quad \square\square\square\square\square\square\square$$

Where index i represents to y and j represents to time t, $\Delta t = t_{j+1} - t_j$ and$\Delta y = y_{j+1} - y_j$. Getting the values of u, θ and C at time t, we may compute the values at time $t + \Delta t$ as following method: we substitute i = 1, 2, ..., $l-1$, where n correspond to ∞ ,equations 15 to 17 give tridiagonal system of equations with boundary conditions in equation 18, are solved employing Thomas algorithm as discussed in Carnahan et al.[23], we find values of θ and C for all values of y at t + Δt. Equation 15 is solved by same to substitute these values of θ and C, we get solution for u till desired time t.

IV. ANALYSIS ON OBTAINED RESULTS

In this study, the Soret and Dufour effect is used to investigate the boundary layer unsteady MHD Jeffery flow past a porous vertical plate. The mass diffusion equation now includes the first order chemical reaction's influence. Skin friction coefficients, Nusselt number, and Sherwood number are presented with the use of tables, while numerical results of velocity profile u, temperature profile, and concentration profile C have been discussed with the aid of graphs in order to see a physical view of the work.
The following values are used for investigation
Gr = 3, Gm = 6, K = 0.8, M = 2, Pr = 0.7, Du = 0.5, Sc = 0.4, Sr = 2, R = 1.5, Kr = 0.7, t = 0.1.
It is noted from figure 5 that increasing radiation parameter R, velocity u decreases. It is analyzed that an increase in R, temperature θ increases in figure 13 and it is notable that an increase in R, concentration C near to plate decrease after that increases in figure 22. In figure 4, velocity decreases as Prandtl number Pr increases while temperature and concentration decreases in figure 12 and 18 respectively when Pr increases. Figure 20, depicts the variation of Schmidt number Sc as concentration decreases rapidly with increase Sc while velocity profile in figure 7 decreases near to plate. In figure 1, 16 and 10, it is seen that velocity increases and increases slowly after sometime; and concentration decreases as increase Dufour number Du, whereas temperature increases rapidly as Du increases. Figures 6, 14 and 19 depict the behavior of chemical reaction parameter Kr on velocity, temperature and concentration decreases respectively. It is seen that velocity decreases, temperature and concentration decreases rapidly as Kr increase. Figure 9, 15 and 23 reveals that velocity, temperature and concentration increase on increase of time. Figure 8 and 21 depict that increment in Soret number Sr, velocity and concentration increases respectively.

The effect of Jeffery fluid parameter λ can be seen in figures 2 and 24, velocity profile and concentration profile decreases on increase of Jeffery fluid parameter. Effect of magnetic parameter M can seen in figure 3, 11 and 17 for velocity, temperature and concentration, they all decreases on increase of magnetic parameter ,Velocity decreases slowly while temperature and concentration decreases rapidly.

It is observed from **Table 1** that Change in Schmidt number Sc effects as skin friction coefficient and Nusselt number decreases while Sherwood number increases. Pr effects as skin friction coefficient and Sherwood number Sh decrease while Nusselt number increases. Sherwood number Sh increase whereas Skin friction coefficient and Nusselt number decreases with Dufour number Du increases. Increase in Soret number Sr, Skin friction and Sherwood number Sh increase while Nusselt number Nu decreases. On increasing Jeffery fluid parameter λ results in Sherwood number Sh increases and Nusselt number Nu decreases. It is also noted that on increasing magnetic parameter M, Skin friction and Nusselt number Nu decreases while Sherwood number Sh increases. Skin friction and Nusselt numbers decreases while Sherwood number Sh increases on increase of radiation parameter R. The effect of chemical reaction parameter Kr can be seen that skin friction and Nusselt number Nu decreases while Sherwood number Sh increases on increasing chemical reaction parameter Kr.

V. CONCLUSION

On an unsteady MHD Jeffery flow over a vertical porous plate submerged in a porous material, the impacts of first order chemical reactions and changes in Soret-Dufour effects are examined. These findings from the inquiry are as follows:

.

5.1 The effect of radiation on concentration is noteworthy. It is observed that increasing values of R, concentration falls down and after some distance from the plate, it goes up slowly-slowly while velocity decreases and temperature increases.

5.2 Interestingly, decrement in concentration has been found on increasing Prandtl number Pr while temperature decreases rapidly.

5.3 For increasing values of Kr, it is a considerable enhancement in velocity, i.e. velocity decreases slowly but concentration decreases rapidly.

5.4 Increasing values of Dufour number, it is observed that temperature profile in the thermal boundary layer and concentration decreases in the boundary layer.

5.5 Schmidt number greatly influences the concentration profile in the concentration boundary layer.

5.6 On increasing Jeffery fluid parameter λ , velocity and concentration decreases slowly.

Figures have been shown below with the variation of different flow parameters.

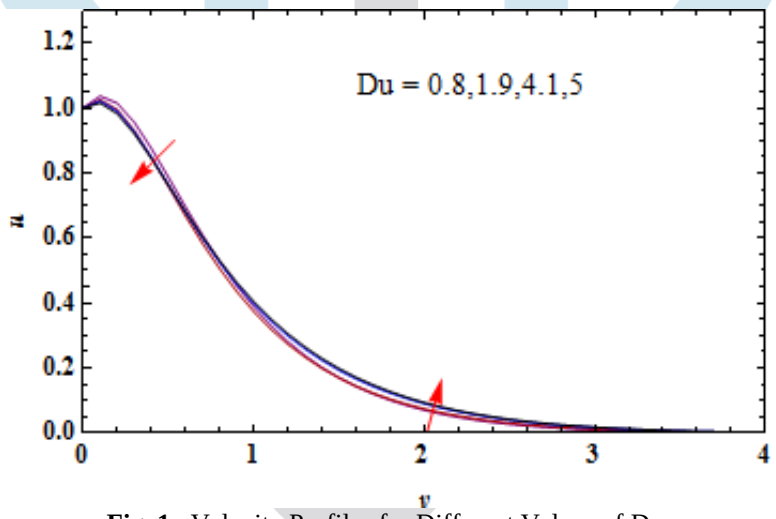

Fig. 1 Velocity Profiles for Different Values of Du

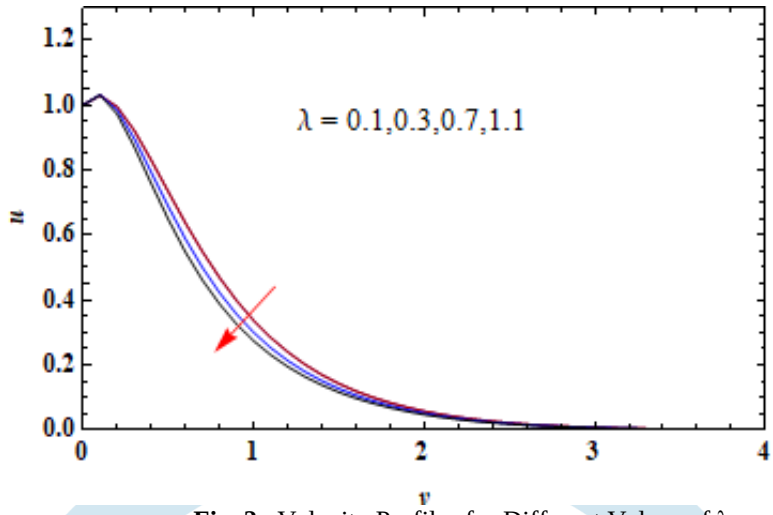

Fig. 2 Velocity Profiles for Different Values of λ

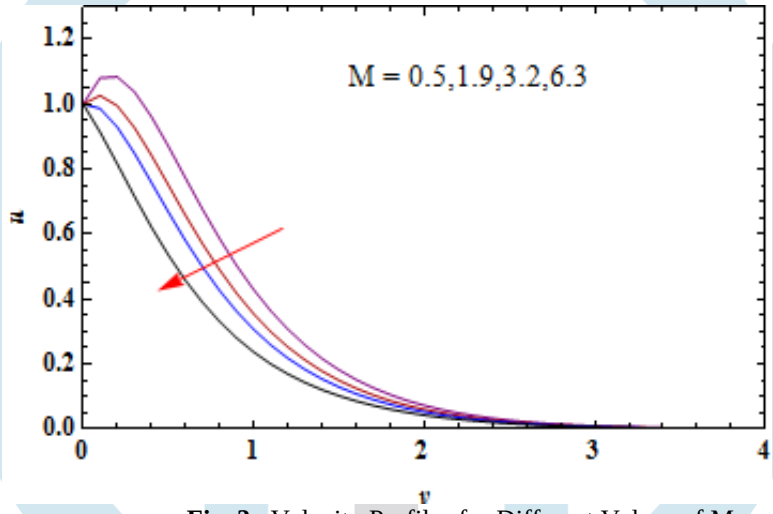

Fig. 3 Velocity Profiles for Different Values of M

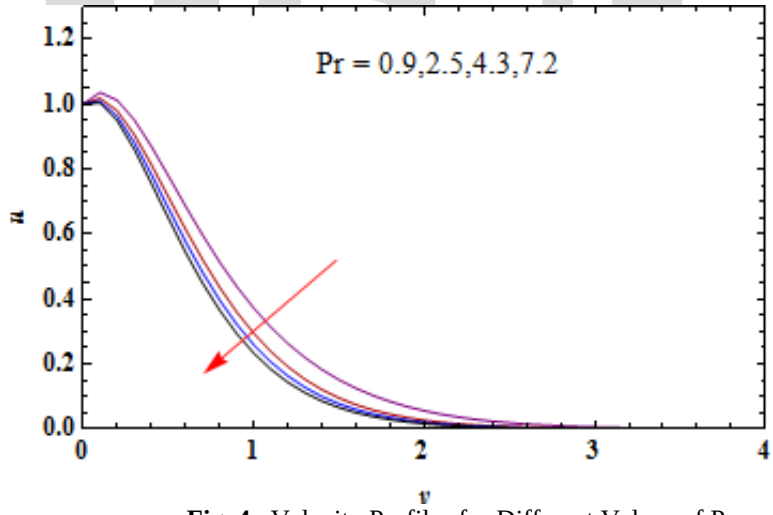

Fig. 4 Velocity Profiles for Different Values of Pr

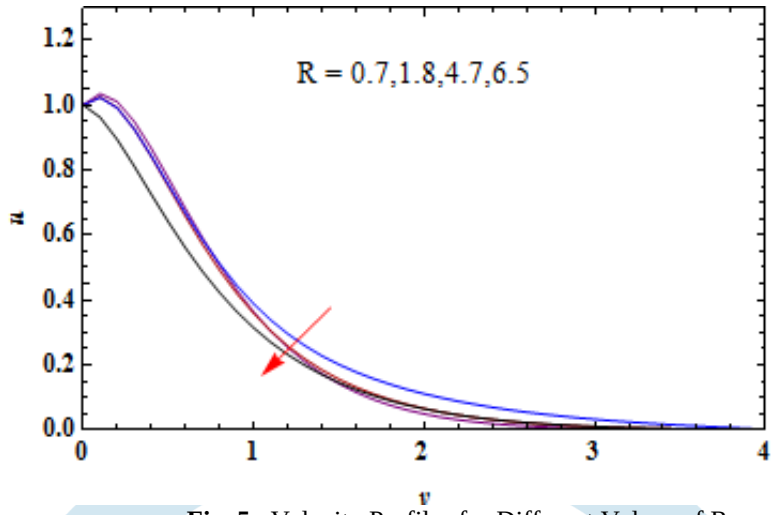

Fig. 5 Velocity Profiles for Different Values of R

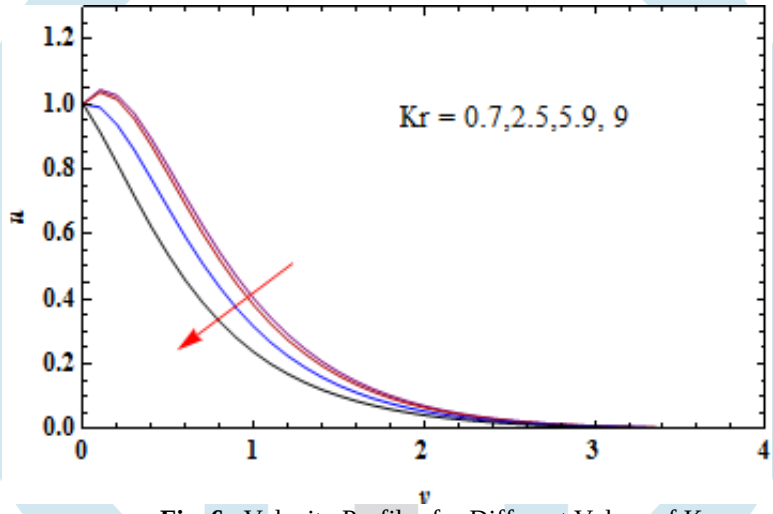

Fig. 6 Velocity Profiles for Different Values of Kr

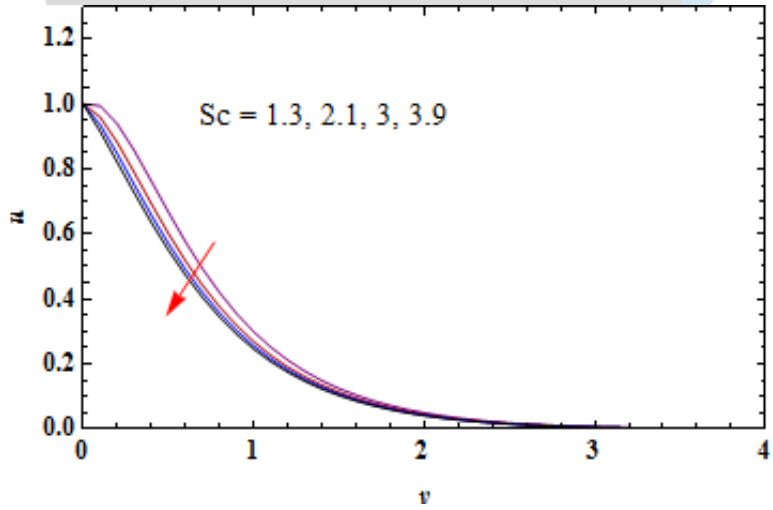

Fig. 7 Velocity Profiles for Different Values of Sc

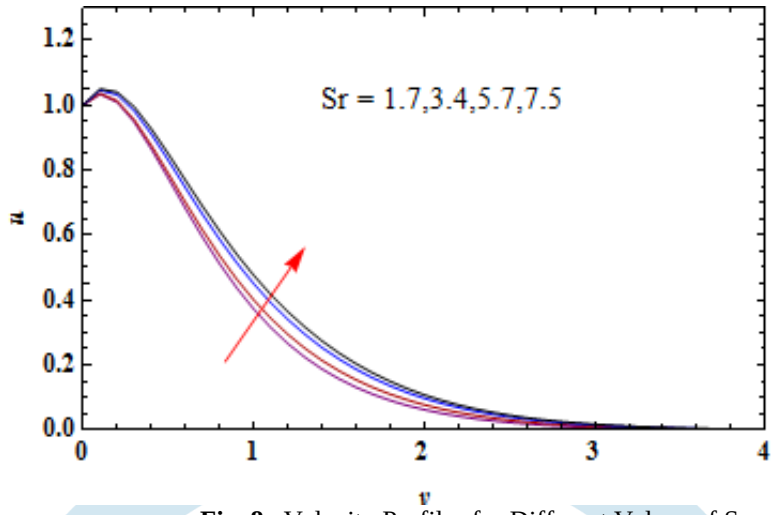

Fig. 8 Velocity Profiles for Different Values of Sr

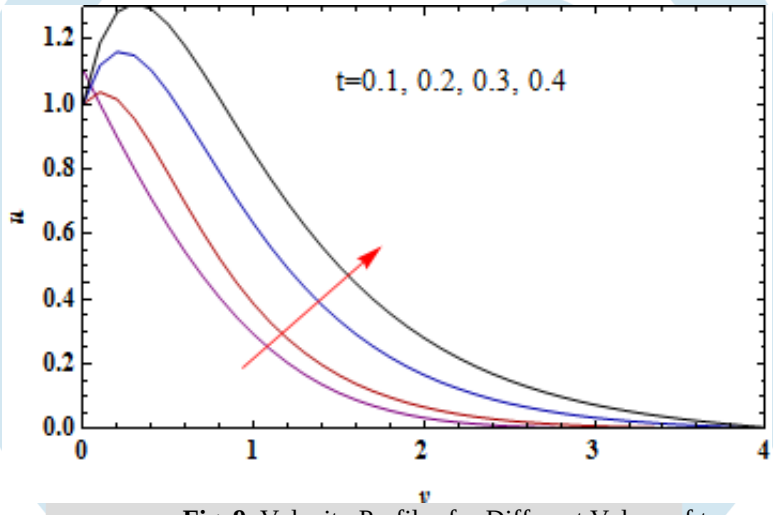

Fig. 9 Velocity Profiles for Different Values of t

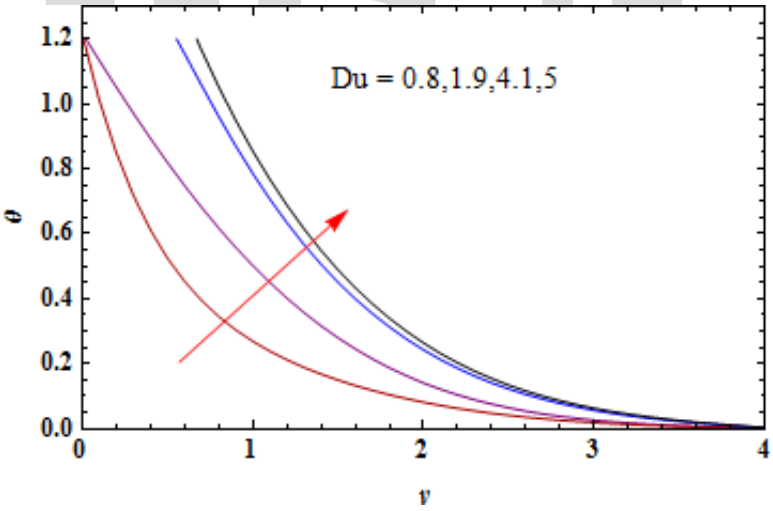

Fig. 10 Temperature Profiles for Different Values of Du

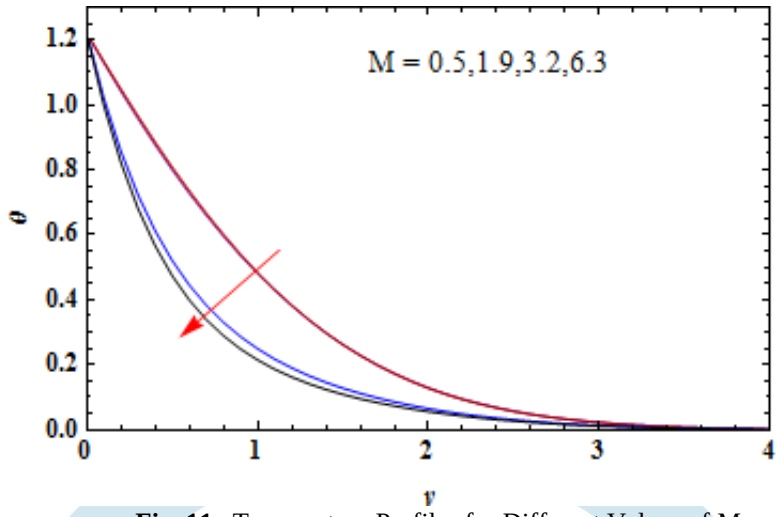

Fig. 11 Temperature Profiles for Different Values of M

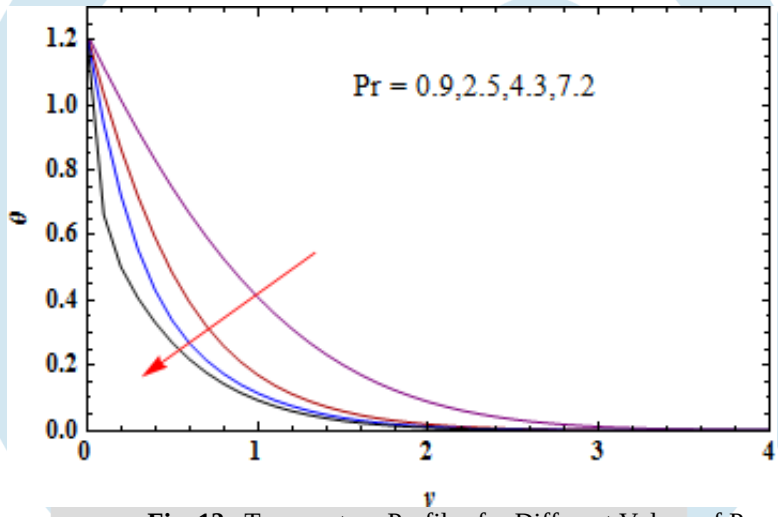

Fig. 12 Temperature Profiles for Different Values of Pr

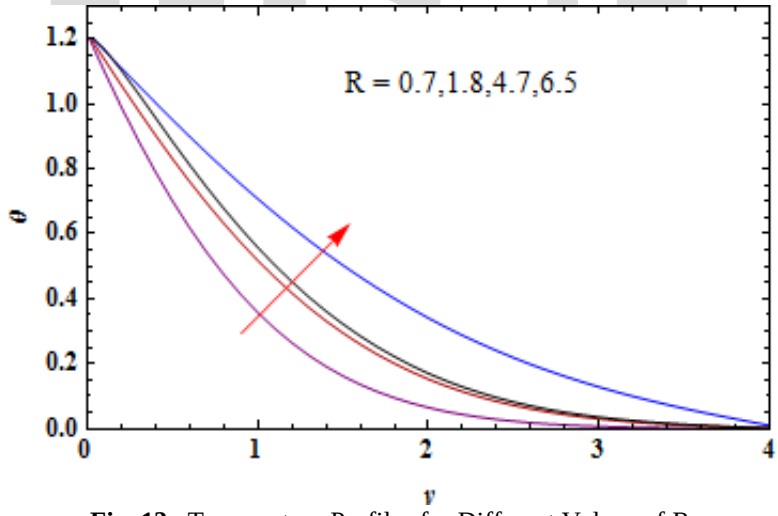

Fig. 13 Temperature Profiles for Different Values of R

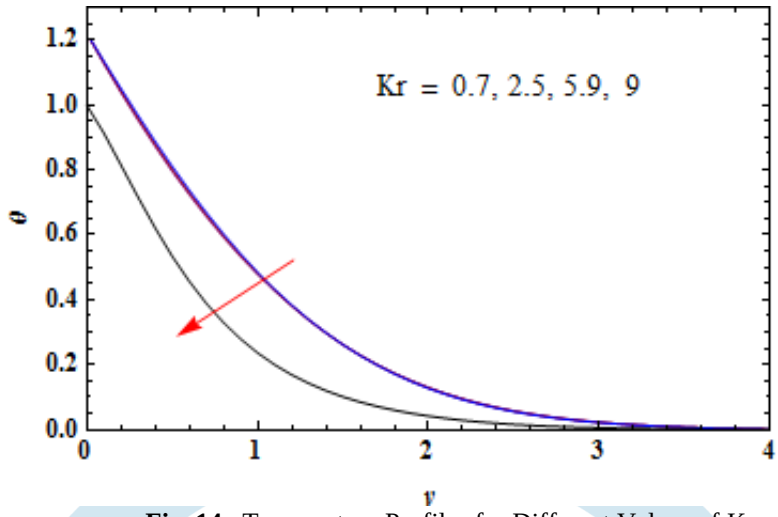

Fig. 14 Temperature Profiles for Different Values of Kr

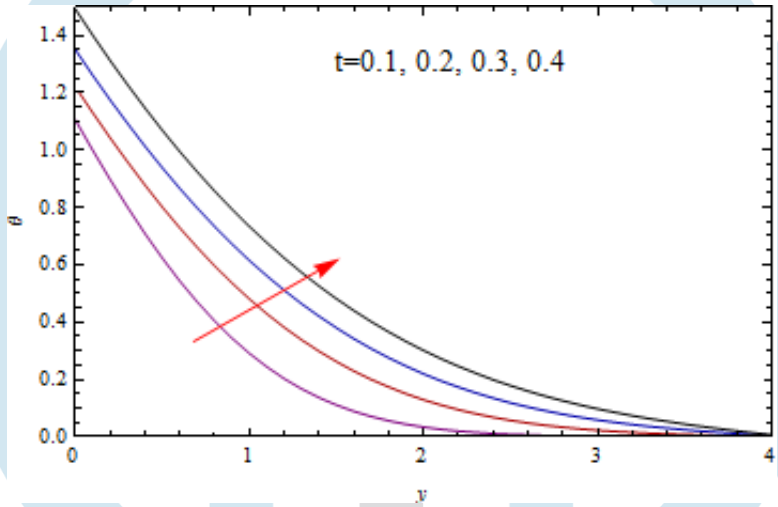

Fig. 15 Temperature Profiles for Different Values of t

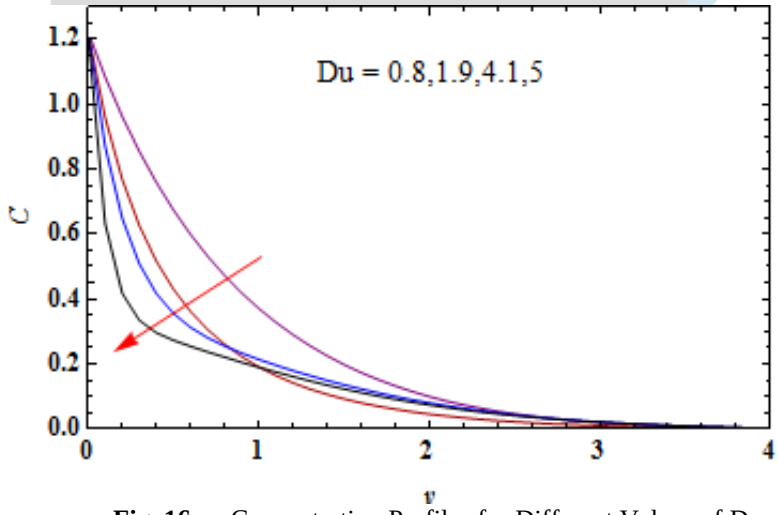

Fig. 16 Concentration Profiles for Different Values of Du

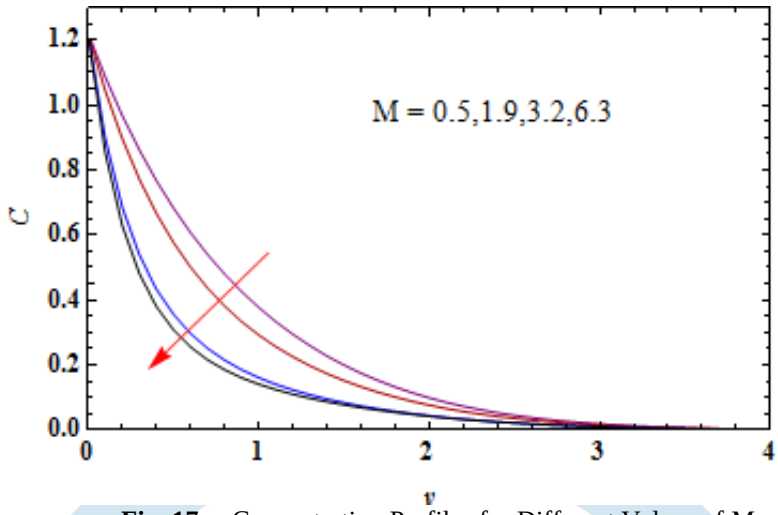

Fig. 17 Concentration Profiles for Different Values of M

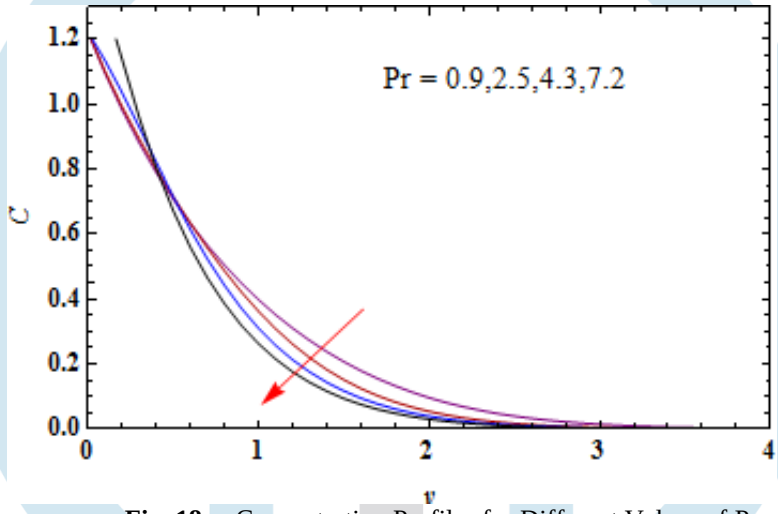

Fig. 18 Concentration Profiles for Different Values of Pr

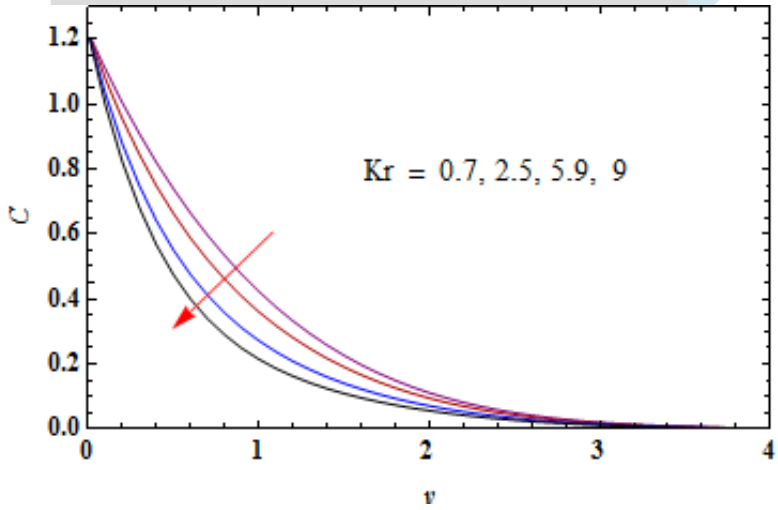

Fig. 19 Concentration Profiles for Different Values of Kr

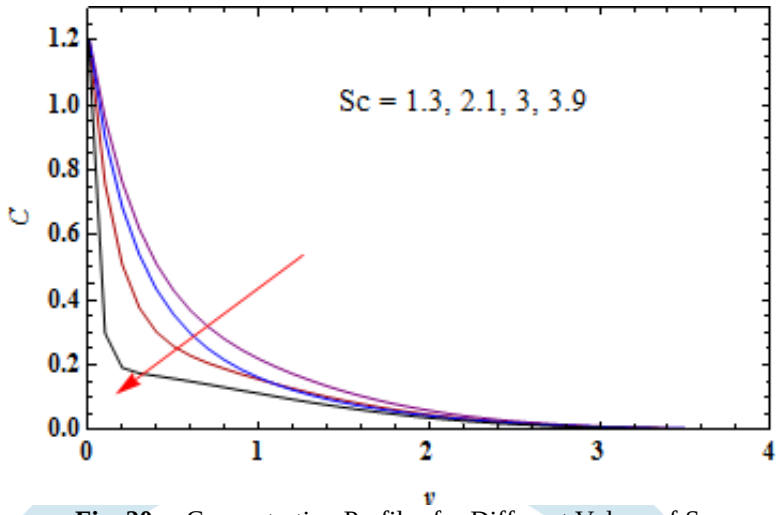

Fig. 20 Concentration Profiles for Different Values of Sc

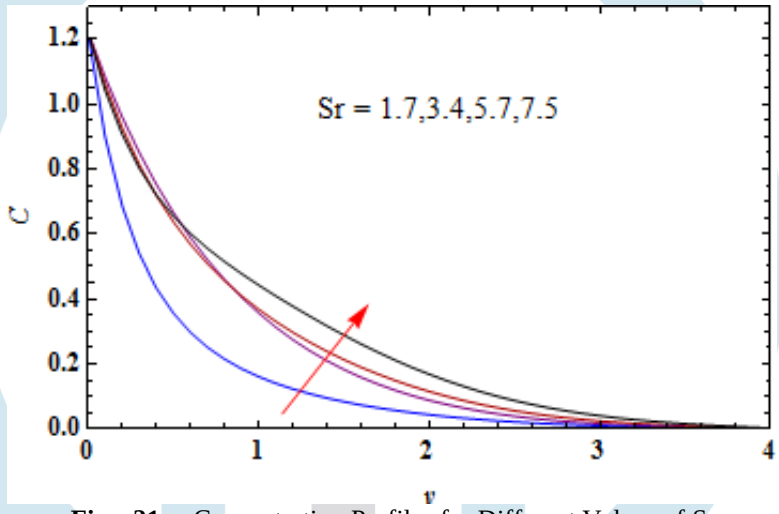

Fige. 21 Concentration Profiles for Different Values of Sr

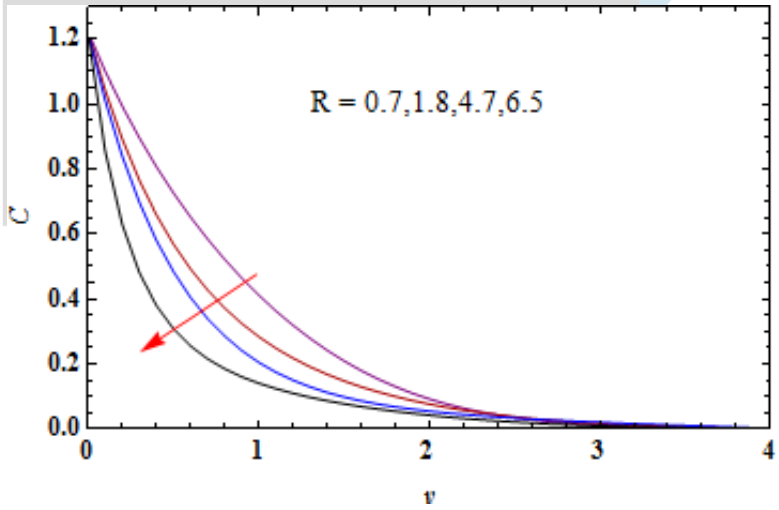

Fig. 22 Concentration Profiles for Different Values of R

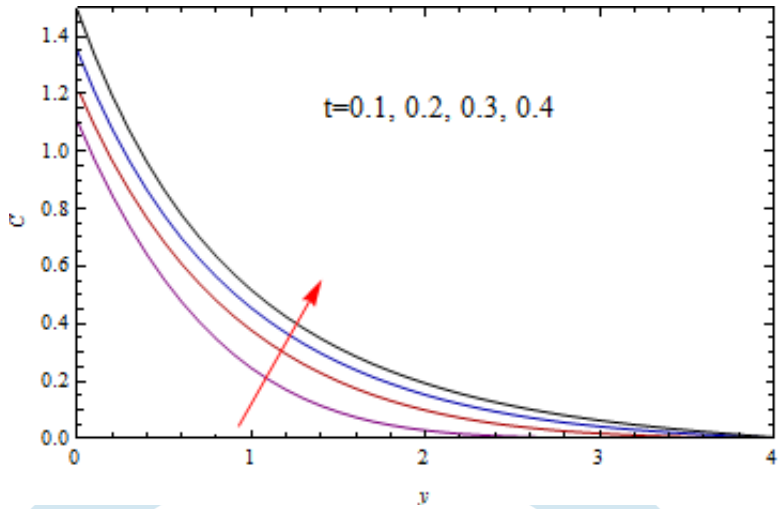

Fig. 23 Concentration Profiles for Different Values of t

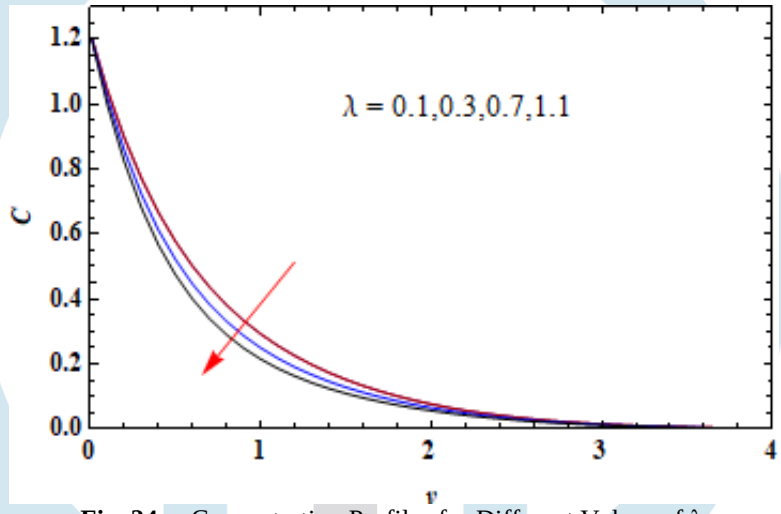

Fig. 24 Concentration Profiles for Different Values of λ

Table 1

Sc	Du	λ	M	Pr	Sr	R	t	Kr	τ	Nu	Sh
1.3	0.5	0.1	2	0.7	2	1.5	0.2	2	-0.052591	0.773531	2.6371
2.1	0.5	0.1	2	0.7	2	1.5	0.2	2	-0.397641	0.554606	4.64747
3	0.5	0.1	2	0.7	2	1.5	0.2	2	-0.63781	0.318407	6.76242
3.9	0.5	0.1	2	0.7	2	1.5	0.2	2	-0.837633	0.0375525	9.25398
0.4	0.8	0.1	2	0.7	2	1.5	0.2	2	0.368652	0.847534	1.37787
0.4	1.9	0.1	2	0.7	2	1.5	0.2	2	0.257354	0.376062	2.0382
0.4	4.1	0.1	2	0.7	2	1.5	0.2	2	0.218925	-1.66691	3.51421
0.4	5	0.1	2	0.7	2	1.5	0.2	2	0.155833	-4.89382	5.88491
0.4	0.5	0.1	2	0.7	2	1.5	0.2	2	0.365039	0.911299	1.3419
0.4	0.5	0.3	2	0.7	2	1.5	0.2	2	0.295914	0.870773	1.76356
0.4	0.5	0.7	2	0.7	2	1.5	0.2	2	0.313446	0.847329	2.00045
0.4	0.5	1.1	2	0.7	2	1.5	0.2	2	0.308701	0.826175	2.20999
0.4	0.5	0.1	0.5	0.7	2	1.5	0.2	2	0.799279	0.911299	1.3419
0.4	0.5	0.1	1.9	0.7	2	1.5	0.2	2	0.261037	0.870773	1.76356
0.4	0.5	0.1	3.2	0.7	2	1.5	0.2	2	-0.141167	0.847329	2.00045
0.4	0.5	0.1	6.3	0.7	2	1.5	0.2	2	-0.863401	0.826175	2.20999
0.4	0.5	0.1	2	0.9	2	1.5	0.2	2	0.353249	1.04986	1.26819
0.4	0.5	0.1	2	2.5	2	1.5	0.2	2	0.179236	1.87266	1.21818
0.4	0.5	0.1	2	4.3	2	1.5	0.2	2	0.0914181	2.78975	0.880602
0.4	0.5	0.1	2	7.2	2	1.5	0.2	2	0.0370822	5.58048	-0.900555
0.4	0.5	0.1	2	0.7	1.7	1.5	0.2	2	0.334714	0.906911	1.38647

0.4	0.5	0.1	2	0.7	3.4	1.5	0.2	2	0.354174	0.886626	1.60996
0.4	0.5	0.1	2	0.7	5.7	1.5	0.2	2	0.452321	0.883873	1.65805
0.4	0.5	0.1	2	0.7	7.5	1.5	0.2	2	0.492931	0.872001	1.79427
0.4	0.5	0.1	2	0.7	2	0.7	0.2	2	0.345844	1.1714	1.1999
0.4	0.5	0.1	2	0.7	2	1.8	0.2	2	0.242769	0.815036	1.78658
0.4	0.5	0.1	2	0.7	2	4.7	0.2	2	0.232613	0.543516	2.09357
0.4	0.5	0.1	2	0.7	2	6.5	0.2	2	-0.378286	0.505111	3.65307
0.4	0.5	0.1	2	0.7	2	1.5	0.1	2	-0.868317	1.05914	1.35815
0.4	0.5	0.1	2	0.7	2	1.5	0.2	2	0.365039	0.911299	1.3419
0.4	0.5	0.1	2	0.7	2	1.5	0.3	2	1.19186	0.890684	1.43997
0.4	0.5	0.1	2	0.7	2	1.5	0.4	2	1.88882	0.914055	1.57845
0.4	0.5	0.1	2	0.7	2	1.5	0.2	0.7	0.430863	0.931315	1.1278
0.4	0.5	0.1	2	0.7	2	1.5	0.2	2.5	0.368593	0.904029	1.4187
0.4	0.5	0.1	2	0.7	2	1.5	0.2	5.9	-0.10399	0.859912	1.87393
0.4	0.5	0.1	2	0.7	2	1.5	0.2	9	-0.863401	0.826175	2.20999

VI. ACKNOWLEDGMENT

We acknowledge our principal Dr. V. C. Tripathi and chief proctor of science faculty Dr A. K. Dwivedi and thank for encouraging to complete this research work.

REFERENCES

[1] Nadeen S., Akbar N.S., Haq R.U. and Khan Z.H. , "Radiation effect on MHD stagnation point flow of nanofluid towards a stretching surface with convective boundary conditions", Chinese journal of Aeronautics, vol.26 (6), pp.1389–1397, 2013.

[2] Ibrahim S.M., Mabood F, Lorenzini G and Lorenzini E., "Radiation effects on Williamson nanofluid flow over a heated surface with Magnetohydrodynamics", International Journal of Heat and Technology, vol.35 (1), pp.196–204, 2017.

[3] Oztop H.F. and Selimefendigil F., "Analysis of MHD mixed convection in a flexible walled and nanofluids filled lid driven cavity with volumetric heat generation". Int J Mech Sci, vol.118, pp.113–124, 2016.

[4] Kumar S. and Rajput U.S. , "Radiation effect on MHD flow past an impulsively started vertical plate with variable heat and mass transfer", J. Appl Math. Mech., vol.8, pp.66–85, 2012.

[5] Ahmad A., Hayat T., Hina Z. and Anum T., "Soret and Dufour effects on MHD peristaltic transport of jeffery fluid in a curved channel with convective boundary conditions", PLOS ONE, vol.12 (2), 2017.

[6] Katagiri Srihari. , "Soret, Dufour and Hall effects on unsteady MHD flow past a semi infinite vertical plate by the presence of heat source", Journal of international academy of physical sciences, vol.22 (1), pp.25–50, 2018.

[7] Kharabela swain, Sampada K. Parida and Gauranga C. Dash., "Higher order chemical reaction on MHD nanofluid flow with slip boundary conditions: A numerical approach", Mathematical modeling of engineering, vol.6 (2), pp.293–299, 2019.

[8] Anjana Matta, Nagaraju Gajjela. , "Order of chemical reaction and convective boundary condition effects on micropolar fluid flow over a stretching sheet", AIP advances, vol.8 Article ID 115212, 2018.

[9] Halima usman, Ime Jimy Uwanta and Smaila Kanba Ahmad., "Magnetohydrodynamics free convection flow with thermal radiation and chemical reaction effects in presence of variable suction", MATEC Web of Conferences, vol.64, Article ID 01002, 2016.

[10] Rahman M. and Dash M., "Combined effects of internal heat generation and higher order chemical reaction on the non-Darcian forced convective flow of a viscous incompressible fluid with variable viscosity and thermal conductivity over a stretching surface embedded in a porous medium", Can. J. Chem. Eng., vol.90, pp.1631–1644, 2012.

[11] T. Hayat, G. Bashir, M. Waqas, A. Alsaedi, "MHD flow of Jeffrey liquid due to a nonlinear radially stretched sheet in presence of Newtonian heating", Results in Physics, vol. 6, pp.817–823, 2016.

[12] M. Eswara Rao, S. Sreenadh, "MHD Boundary Layer Flow of Jeffrey Fluid over a Stretching/Shrinking Sheet through Porous Medium", Global Journal of Pure and Applied Mathematics, vol.13(8), pp.3985-4001, 2017.

[13] T. Hayat, R. Sajjad Saif, R. Ellahi, T. Muhammad, A. Alsaedi, "Simultaneous effects of melting heat and internal heat generation instagnation point flow of Jeffrey fluid towards a nonlinear stretching surface with variable thickness", International Journal of Thermal Sciences, vol.132, pp.344–354, 2018.

[14] M.A. Rana, Y. Ali, M. Shoaib, "Three-dimensional Couette flow of a Jeffrey fluid along periodic injection/suction", Arabian Journal of Mathematical Sciences, vol.7, pp.229–247, 2018.

[15] M.A. Imran, F. Miraj, I. Khan, I. Tlili, "MHD fractional Jeffrey's fluid flow in the presence of thermo diffusion, thermal radiation effects with first order chemical reaction and uniform heat flux", Results in Physics, vol.10, pp.10–17, 2018.

[16] T. Hayat, S. Asad, A. Alsaedi, F.E. Alsaad, "Radiative Flow of Jeffrey Fluid Through a Convectively Heated Stretching Cylinder", Journal of Mechanics, vol.31(1), pp.69-78, 2015.

[17] K. Das, N. Acharya, P. Kumar Kundu, "Radiative flow of MHD Jeffrey fluid past a stretching sheet with surface slip and melting heat Transfer", Alexandria Engineering Journal, vol.54(4), pp.815–821, 2015.

[18] M.M. Bhatti, M. Ali Abbas, "Simultaneous effects of slip and MHD on peristaltic blood flow of Jeffrey fluid model through a porous Medium", Alexandria Engineering Journal, vol.55(2), pp.1017–1023, 2016.
[19] S. Sreenadh, K. Komala, A.N.S. Srinivas, "Peristaltic pumping of a power – Law fluid in contact with a Jeffrey fluid in an inclined channel with permeable walls", Ain Shams Engineering Journal, vol.8(4), pp.605–611, 2017.
[20] S. Farooq, M. Awais, M. Naseem, T. Hayat, B. Ahmad, "Magneto hydrodynamic peristalsis of variable viscosity Jeffrey liquid with heat and mass transfer", Nuclear Engineering and Technology, vol.49(7), pp.1396-1404, 2017.
[21] K. Venkateswara Raju, A. Parandhama, M.C. Raju, K. Ramesh Babu, "Unsteady MHD Mixed Convection Flow of Jeffrey Fluid Past a Radiating Inclined Permeable Moving Plate in the Presence of thermophoresis Heat Generation and Chemical Reaction", Journal of Ultra Scientist of Physical Sciences, vol.30(1), 51-65, 2018.
[22] D. Dastagiri Babu, , S. Venkateswarlu, E. Keshava Reddy, "Multivariate Jeffrey Fluid Flow past a Vertical Plate through Porous Medium, J. Appl. Comput. Mech., vol.6(3), pp.605-616, 2020.
[23] Brice Carnahan, H.A. Luther and James O. Wilkes. , Applied Numerical Methods, Krieger Pub Co, 1990, Florida.